

Exchange Bias Properties Using Antiferromagnetic Heusler Alloys: Ni₂MnAl and Mn₂VAl

著者	TSUCHIYA TOMOKI
学位授与機関	Tohoku University
学位授与番号	甲第18125号
URL	http://hdl.handle.net/10097/00125243

氏名	つちや ともき 土屋 朋生
研究科, 専攻の名称	東北大学大学院工学研究科 (博士課程) 知能デバイス材料学専攻
学位論文題目	Exchange Bias Properties Using Antiferromagnetic Heusler Alloys: Ni ₂ MnAl and Mn ₂ VAl
論文審査委員	主査 東北大学教授 高梨 弘毅 東北大学教授 杉本 諭 東北大学教授 新田 淳作 東北大学准教授 角田 匡清

論文内容要約

Chapter 1: Introduction

Ir-Mn is the most utilized antiferromagnet in spin-valve structures. However, Ir is the rarest element and it is unsuitable for generic devices in terms of element strategy. To replace Ir-Mn, antiferromagnetic Heusler alloys are focused on as candidate materials in this study. Antiferromagnetic Heusler alloys have the same structure as half-metallic Heusler alloys, which enable the epitaxial growth of the layered structure including the antiferroferromagnetic/ half-metallic Heusler alloys for any crystal plane. Furthermore, antiferromagnetic Heusler alloys can be prepared without rare elements. The antiferromagnetic Heusler alloys studied in this paper are Ni₂MnAl and Mn₂VAl. Ni₂MnAl showed antiferromagnetism with the Neel temperature of 313 K when it was B2 phase. Mn₂VAl showed antiferromagnetism with a Neel temperature of about 600 K when it was A2-like phase with a small amount of B2 or L2₁ phase, which is confirmed by the temperature dependence of magnetization (M - T curve) and the neutron diffraction for bulk experiments. On the other hand, the antiferromagnetism of Mn₂VAl has not been reported for film samples.

However, the systematical investigation of the exchange bias using antiferromagnetic Heusler alloys has been still lacking. From these backgrounds, objective of this study is the systematical investigation of the exchange bias properties using antiferromagnetic Heusler alloys to obtain the guideline for realizing the large exchange bias shift (H_{ex}) and the high blocking temperature (T_B) using antiferromagnetic Heusler alloys.

Chapter 2: Experimental procedures

The film samples were deposited on 0.5-mm-thick MgO(100) single-crystal substrates using ultra-high-vacuum magnetron sputtering technique. Representative stacking structures were Al (3 nm)/FM (3 nm)/Ni₂MnAl (100 nm)/MgO(100) substrate and Ta (3 nm)/Fe (3 nm)/Mn₂VAl (100 nm)/MgO(100) substrate. The Ni₂MnAl and Mn₂VAl layers were deposited by co-sputtering technique with pure Ni, Mn, Al targets and an alloy target, respectively. The film compositions were confirmed to be stoichiometric composition for both systems. Some samples were annealed in a magnetic field of 1 T for 30 minutes to induce the exchange bias. The crystal structures were characterized using X-ray diffraction (XRD) and a transmission electron microscopy (TEM). Magnetic properties were characterized by a vibrating sample magnetometer (VSM), nuclear magnetic resonance (NMR) and neutron diffraction.

Chapter 3: Exchange bias properties in Ni₂MnAl/FM (FM: Fe, Co, Co₂MnSi) bilayers

In this chapter, the annealing temperature (T_{anneal}) dependence and the ferromagnetic (FM) layer dependence on the exchange bias properties of Ni₂MnAl were reported. In addition, the training effect and the sign reversal of the exchange bias shift were also discussed.

Epitaxially grown B2-Ni₂MnAl films were successfully fabricated on MgO(100) single crystal substrate with 001 orientation. The order parameter of B2 phase was almost 0.6 and it showed no dependence on the T_{anneal} and FM materials. The measurement temperature (T_{measure}) dependence of the H_{ex} and the T_{B} as a function of the T_{anneal} for Ni₂MnAl/Fe bilayers were shown in Figure 1 and Figure 2, respectively. The exchange bias was observed at low temperature and the H_{ex} drastically decreased with increasing the T_{measure} . The sign reversal of the exchange bias was observed below the T_{B} . The possible origin of the sign reversal was the training effect, which was confirmed at 10 K. The T_{B} increased with the T_{anneal} and the highest T_{B} was 200 K for $T_{\text{anneal}} = 500^{\circ}\text{C}$, which was close to the Neel temperature of the Ni₂MnAl films. The grain size of Ni₂MnAl also increased with T_{anneal} . Therefore, the increase of T_{B} was probably due to the increase of the grain size. The increase of the T_{B} with the grain size was successfully demonstrated in the antiferromagnetic Heusler alloy system by controlling annealing conditions. The cooling field (H_{FC}) dependence was also investigated in the Ni₂MnAl/Fe bilayer. The exchange bias in the Ni₂MnAl/Fe bilayer was not reversed even at the H_{FC} of 9 T in spite of the antiferromagnetic coupling between Fe and Mn. The T_{B} and the unidirectional anisotropy energy (J_{u}) of Ni₂MnAl/Fe were higher than those of other bilayers. Therefore, Fe was the most appropriate ferromagnetic material among the three investigated in this thesis.

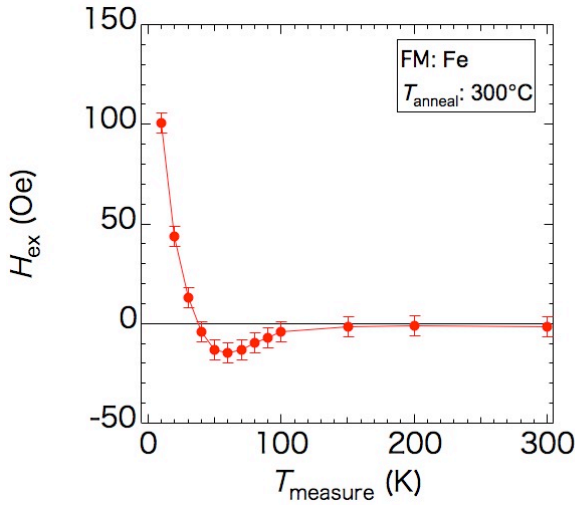


Figure 1: Measurement temperature dependence of the exchange bias shift in Ni₂MnAl/Fe bilayer for $T_{\text{anneal}} = 300^{\circ}\text{C}$

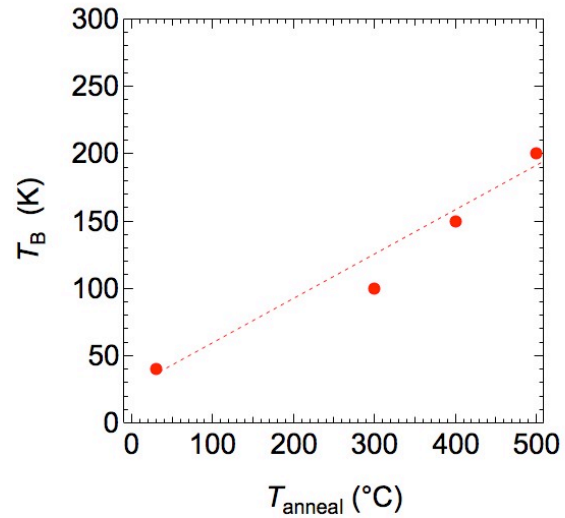


Figure 2: Blocking temperature as a function of the annealing temperature in Ni₂MnAl/Fe bilayers

Chapter 4: Structural, magnetic and transport properties in Mn_2VAl films

In this chapter, the deposition temperature (T_{sub}) dependences on the structural, magnetic transport properties of Mn_2VAl were reported. In addition, the origin of the antiferromagnetism of Mn_2VAl was also discussed.

The T_{sub} dependence of out-of-plane XRD patterns for Mn_2VAl films are shown in Figure 3. All the samples showed 004 fundamental diffraction. The 002 superlattice diffraction from the B2 ordered phase was observed for T_{sub} ranging from 450 to 650°C, for which the (111) superlattice diffractions from the L_{21} ordered phase were also confirmed. These results indicated that the Mn_2VAl samples were L_{21} -phase for the T_{sub} in the range of 450 to 650°C, and the other samples were A2-phase. Magnetization curves of Mn_2VAl films with different T_{sub} are shown in Figure 4. The magnetic field was applied along an in-plane direction and the maximum field was 20000 Oe. The samples deposited below 450°C and above 650°C showed no spontaneous magnetization, on the other hand, those deposited at 450 - 650°C showed hysteresis loops. These results were consistent with the XRD results, and thus the A2-type Mn_2VAl was a paramagnet or an antiferromagnet, and L_{21} -type Mn_2VAl was a ferrimagnet. To identify the magnetism in A2-type Mn_2VAl films, neutron diffraction experiments were performed at RT. A diffraction spot from the antiferromagnetic ordering was observed for $T_{\text{sub}} = 400^\circ\text{C}$, on the other hand, no magnetic reflection spot was observed for $T_{\text{sub}} = \text{RT}$. These results suggested that the Mn_2VAl film is antiferromagnetic for $T_{\text{sub}} = 400^\circ\text{C}$, and paramagnetic for $T_{\text{sub}} = \text{RT}$. To characterize the magnetism of Mn_2VAl films, nuclear magnetic resonance (NMR) experiments were also performed. NMR experiments revealed that the ferrimagnetic, antiferromagnetic and paramagnetic phases were coexisted in the sample for $T_{\text{sub}} = 400^\circ\text{C}$. Although both samples were A2 phase from the results of XRD and neutron diffraction, the antiferromagnetism for $T_{\text{sub}} = 400^\circ\text{C}$ was considered to originate from partially ordered phases, which were confirmed by TEM observation. According to the first principles calculations, spin moments of Mn and V atoms at anti-sites antiparallel coupled with those at original sites. Therefore, there was a possibility to be an antiferromagnetic state when an “optimum low degree of order” is chosen in B2-A2 region. To measure the Neel temperature of the antiferromagnetic Mn_2VAl film, the temperature dependences of the electrical resistivity (ρ - T curves) were measured. A2-type Mn_2VAl films showed the semiconductor like behavior, which the resistivity decreased with increasing the temperature. Antiferromagnets should show the kink around at the Neel temperature, however, no kink was observed in the ρ - T curves in 300-700 K. This was probably due to the small amount of the antiferromagnetic phase in the antiferromagnetic Mn_2VAl film.

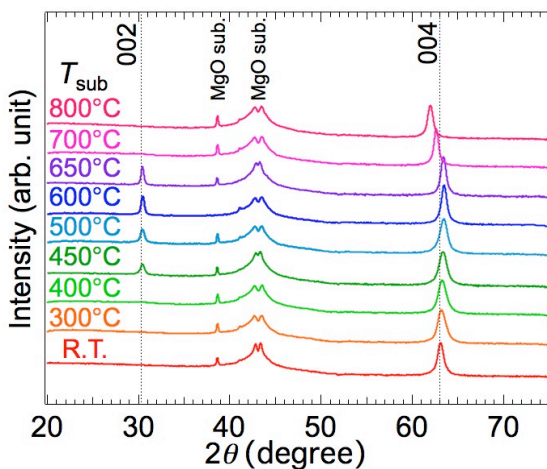


Figure 3: Out-of-plane XRD patterns of Mn_2VAl films with different T_{sub} s

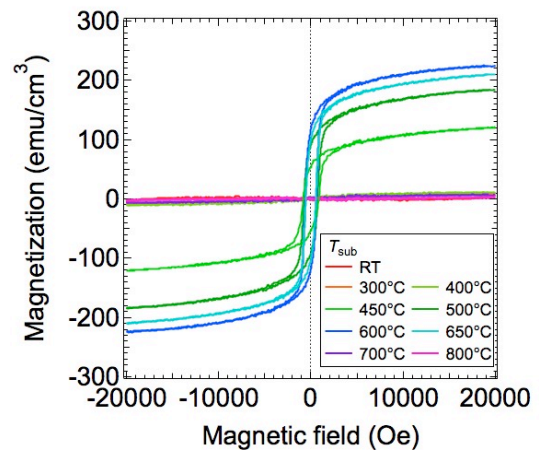


Figure 4: Magnetization curves of Mn_2VAl films with different T_{sub} s

Chapter 5: Exchange bias properties in Mn₂VAl/Fe bilayers

In this chapter, the annealing condition dependences on the exchange bias properties of Mn₂VAl/Fe bilayer was reported.

Magnetization curve of the Mn₂VAl/Fe bilayer for T_{sub} : 400°C measured at RT were shown in Figure 5. The exchange bias using Mn₂VAl was observed at 300 K, for the first time in the world, suggesting that the T_{B} was higher than 300 K. The T_{sub} dependence of the exchange bias field, H_{ex} , at 10 K was plotted in Figure 6. The H_{ex} increased with T_{sub} in the range of RT-400°C probably due to the increase in the volume fraction of partially ordered phases showing antiferromagnetism in Mn₂VAl, which was suggested by the TEM observation. For $T_{\text{sub}} = 450\text{-}700^\circ\text{C}$, although the samples were ferrimagnetic, small exchange bias shifts were observed. The results suggested that there was a possibility of the existence of an antiferromagnetic phase at the L2₁-type Mn₂VAl/Fe interface. For $T_{\text{sub}} = 800^\circ\text{C}$, no exchange bias shift was observed. This was probably due to an off-stoichiometry of the Mn₂VAl layer caused by Mn sublimation during deposition at the high T_{sub} . The *in situ* annealing temperature dependence of the exchange bias showed the similar trend to the T_{sub} dependence. The effect of *ex-situ* annealing in a magnetic field was also investigated. The blocking temperature increased with increasing the annealing temperature although the exchange bias shift decreased probably due to the inter-diffusion. The thickness dependence of the exchange bias was investigated and the critical thickness was found to be 20 nm. The maximum T_{B} of Mn₂VAl was about 300 K, which was about a half of the Neel temperature of a bulk sample. The possible origin of the difference between the Neel temperature and the blocking temperature was the small volume fraction of the antiferromagnetic phase in the Mn₂VAl film, which led the low Neel temperature of the film.

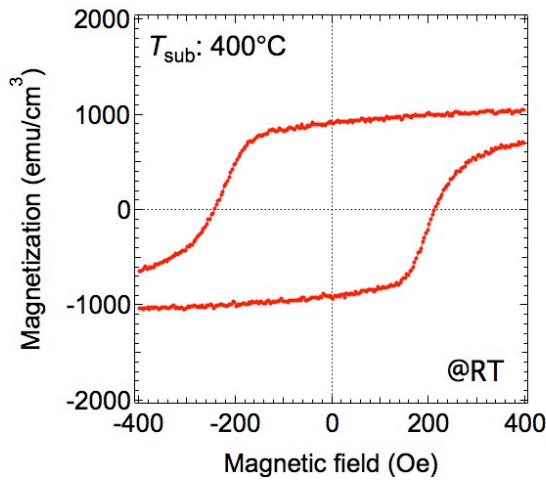


Figure 5: Magnetization curve of a Mn₂VAl/Fe bilayer measured at RT

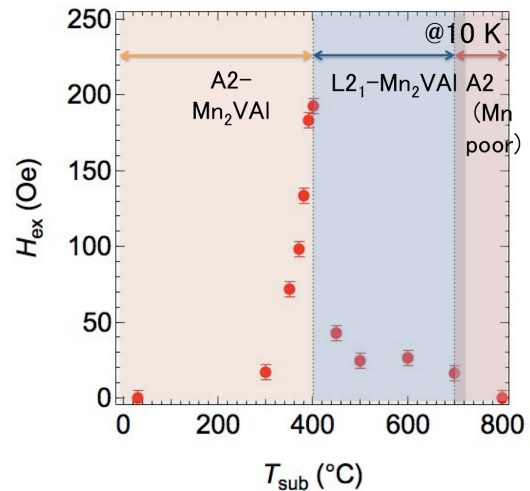


Figure 6: T_{sub} dependence of H_{ex} at 10 K

Chapter 6: Conclusions and perspectives

This thesis demonstrated the exchange bias of antiferromagnetic Heusler alloys. The increase of the T_{B} with the grain size was successfully demonstrated in Ni₂MnAl/FM bilayers by controlling annealing conditions. Antiferromagnetic Mn₂VAl showed the T_{B} of 300 K, which was the highest value among the antiferromagnetic Heusler alloys. The results in this thesis show a high potential of antiferromagnetic Heusler alloys as a new Heusler-type antiferromagnet for the exchange bias system.